

## Topological phase transitions and a spin-related metallic state in inverted HgTe quantum wells under in-plane magnetic field

Maciej Kubisa  and Krzysztof Ryczko \*

*Department of Experimental Physics, Faculty of Fundamental Problems of Technology,  
Wrocław University of Science and Technology, Wybrzeże Wyspiańskiego 27, 50-370 Wrocław, Poland*



(Received 16 July 2021; accepted 4 October 2021; published 18 October 2021)

We show that in inverted HgTe quantum wells, the application of a strong in-plane magnetic field restores the normal sequence of the subbands, thus transforming the system from a topological insulator into a normal insulator phase. The transformation consists of two consecutive quantum phase transitions due to the large Zeeman splitting of electron states. On the other hand, due to the negligible Zeeman splitting of hole states, the intermediate phase between the transitions is semimetallic. Both phase transitions and the semimetallic phase have already been observed, and our theory allows for a consistent interpretation of the experimental results.

DOI: [10.1103/PhysRevB.104.L161406](https://doi.org/10.1103/PhysRevB.104.L161406)

A magnetic field is one of the most effective tools for studying electronic states in semiconductor heterostructures. Typically, the field is directed perpendicular to the layers and splits the two-dimensional subbands into Landau levels, which results in a variety of quantum oscillation phenomena. The effect of an in-plane field is not that striking as the continuous structure of electronic states remains intact. The subbands are only diamagnetically shifted by the energy  $\Delta E_o = \hbar^2/2m^*L^2$  (where  $L = \sqrt{\hbar c/eB}$  is the magnetic length) and spin-split by  $\Delta E_S = g^* \mu_B B$  (where  $\mu_B$  is the Bohr magneton) [1]. In typical heterostructures (such as, e.g., GaAs quantum wells) the changes are small and quite difficult to measure. In contrast, in HgTe quantum wells, both  $\Delta E_o$  and  $\Delta E_S$  have values comparable to the intersubband energies. This is due to the low mass  $m^*$ , the large  $g$ -factor  $g^*$  of the electrons, as well as the small energy gaps between the subbands. Therefore, the in-plane field significantly affects the subband energies and can even change their order. As we will show, this leads to unexpected physical phenomena.

The current interest in HgTe quantum wells was initiated by the work of Bernevig *et al.* [2], who predicted the presence of a topological insulator (TI) phase in these structures. This phase of matter is characterized by a band gap for the bulk states and dissipationless gapless edge states. TI systems can be expected in materials where the conduction and valence bands have opposite parity and their normal order is reversed. The HgTe quantum well is such a material, due to the competition between the barrier ( $\text{Hg}_{1-x}\text{Cd}_x\text{Te}$  with a normal band sequence) and the well (HgTe with an inverted band structure). For small well widths  $d$ , barriers prevail and the system is a normal insulator (NI). But when  $d$  exceeds a certain critical value  $d_c$ , the well material starts to dominate and the valence subband is inverted above the conduction subband. This leads to the formation of the TI phase, which has been confirmed experimentally [3]. At a critical width the

band gap is closed, and the dispersion of crossing conduction and valence subbands shows Dirac cones with massless Dirac fermions [4]. The electric field [5], pressure [6], and temperature [7] affect the value of  $d_c$  and have been proposed as effective tools for inducing transitions between NI and TI phases and for generating the gapless state.

The effect of an in-plane magnetic field on electron transport in the TI phase was first investigated by Gusev *et al.* [8]. They measured the magnetoresistance of an 8-nm HgTe quantum well in fields up to 12 T. A strong decrease of the local resistance combined with a complete suppression of the nonlocal resistance was observed in the fields of about 10 T and was attributed to the phase transition from the TI state to a two-dimensional (2D) metallic state. This supposition was later confirmed by Raichev [9], who calculated the energy spectra of quantum-well states and showed that in-plane fields of the order of 10 T close the band gap. However, the nature of the metallic (more specifically semimetallic) state has not been clarified. Subsequent studies [10] led the authors to conclude that a further increase of  $B$  (above 10 T) does not open the gap and the system remains metallic even in the highest fields. However, recent investigations [11] have revealed that in fields of around 30 T the local resistance increases again, while the nonlocal resistance remains suppressed. This suggests another phase transition, this time from the metallic state to a NI state. Nevertheless, based on the conclusions of Ref. [10], this simple interpretation was rejected by the authors [11].

In this Letter, we demonstrate that the changes in resistance observed by Khouri *et al.* [11] at high magnetic fields are due to the metal-insulator transition. The transition occurs because the in-plane field reopens the band gap and restores the normal sequence of the subbands. Our calculations show that the high-field transition has the same origin as the TI-metal transition observed in lower fields and both take place when the spin-split electron subbands cross the hole subbands. In the intermediate range of fields between the transitions, the

\*krzysztof.ryczko@pwr.edu.pl

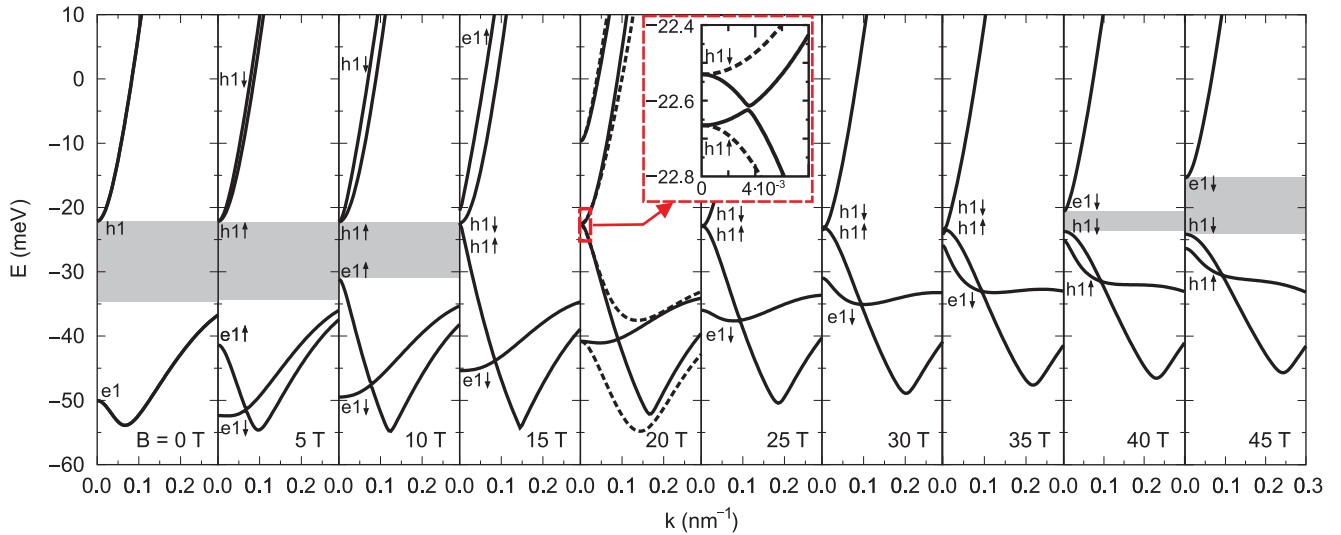


FIG. 1. Evolution of the quantum-well energy spectrum with increasing magnetic field. The calculations have been performed for the 8-nm HgTe well grown in the [001] direction and  $\vec{k} \parallel \vec{B} \parallel [100]$  (an example spectrum for  $\vec{k} \perp \vec{B}$  is shown with dashed lines). The band gaps are marked by shaded areas. The in-plane field closes the gap at  $B \approx 15$  T and reopens at  $B \approx 35$  T. The inset shows that in the closed-gap region the band gap is really zero.

system becomes semimetallic because the spin-degenerated hole subbands act as both conduction and valence subbands.

The energy spectrum of HgTe quantum wells has been calculated on the basis of the  $8 \times 8$  Kane model [12–14], which has also included the effect of uniaxial strain due to the lattice mismatch between barrier and well materials. Material parameters for calculations have been taken from Refs. [6,13,15–21]. To take into account the in-plane field  $\vec{B} = [B_x, B_y, 0]$ , the wave vector  $\vec{k}$  in the Hamiltonian was replaced by  $\vec{k} + (e/\hbar c)\vec{A}$ , where  $\vec{A} = [B_y z, -B_x z, 0]$  is the vector potential. The eigenstate problem for the Kane Hamiltonian has been solved numerically using the finite difference method. The method of calculation is presented in greater detail in the Supplemental Material [22]. All numerical results presented below are for HgTe/Cd<sub>0.65</sub>Hg<sub>0.35</sub>Te quantum wells with different widths grown in the [001] direction (critical width is  $d_c = 6.3$  nm) and subjected to a magnetic field along the [100] axis.

Figure 1 shows the evolution of quantum well subbands in the in-plane magnetic field, calculated for the 8-nm structure. The band gap between the conduction and valence subbands (marked as a shaded region) changes as  $B$  increases and goes through the following steps: (i) In low fields ( $B < 14$  T) the magnetic field gradually reduces the energy gap to zero; (ii) the gap remains closed up to the field of 35 T; and (iii) even greater magnetic fields ( $B > 35$  T) open the gap again. Thus, both in the weak and strong fields, the system is an insulator, while in the intermediate region (ii) it becomes a semimetal. In the regions (i) and (ii), our results are consistent (also quantitatively) with the calculations of Gusev *et al.* [10]. High-field region (iii) was not considered in Ref. [10].

In the low-field region (i), the band gap shown in Fig. 1 is indirect due to the  $k \neq 0$  valence-band maxima, which for small  $B$  exceed the  $k = 0$  maximum. The energy of the side maximum is shown by the dotted line in Fig. 2. The indirect gap decreases with increasing well width  $d$ . For  $d > 11$  nm,

the side maximum overlaps the conduction subband and the system becomes semimetallic at  $B = 0$  [6]. Such wide wells will not be considered here.

Figure 1 suggests that in the region (ii) the topmost valence subband and lowest conduction subband (denoted by  $h1\uparrow$  and  $h1\downarrow$ , respectively) are degenerated at  $k = 0$ . However, closer examination (see the inset) reveals that at  $k = 0$  they are separated by a small gap of about 0.1 meV. Nevertheless, the band gap remains closed due to the subband anticrossing at  $k > 0$ . Note that under the influence of the in-plane field, the subbands become anisotropic, as shown in Fig. 1 for  $B = 20$  T.

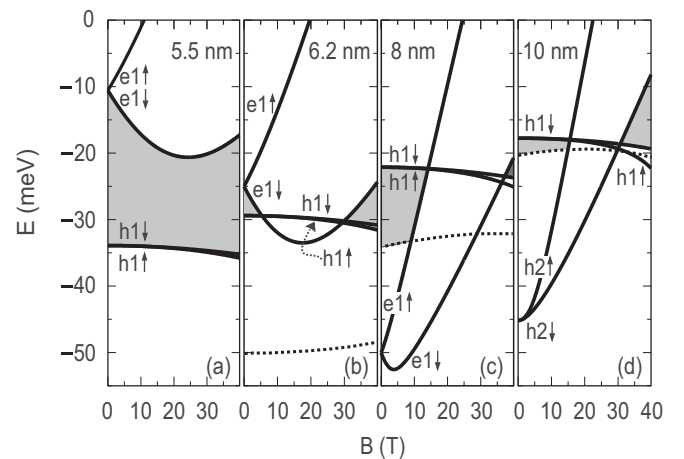


FIG. 2. The  $k = 0$  energies of conduction and valence subbands as functions of the in-plane field, calculated for HgTe quantum wells of different widths. The dotted lines show the positions of the high- $k$  valence-band maxima. The band gaps are marked by shaded areas. In the wells with an inverted band structure, a strong magnetic field restores normal band ordering.

The subbands in Fig. 1 have been identified as electronlike (e) or holelike (h) on the basis of their diamagnetic shift in the in-plane field. This is illustrated in Fig. 2 which shows the subband energies at  $k = 0$  calculated as a function of  $B$  for wells of different widths. The energies in Fig. 2 clearly form two pairs of spin-split levels, of electron type and heavy-hole type. The electron pair, marked as e1, is characterized by a small effective mass (and thus a large diamagnetic shift  $\Delta E_e$ ) and a large  $g$  factor. The hole pair, on the other hand, corresponds to a large (and negative) effective mass and negligible spin splitting. As a result, the levels marked as h1 are weakly field dependent. The evolution of the electron and hole levels in the 8-nm quantum well from Fig. 1 is shown in Fig. 2(c). Since the well width exceeds the critical value, the subbands are inverted ( $h1 > e1$ ) at  $B = 0$ . However, the in-plane field shifts the electron states to higher energies and restores at high  $B$  the normal ( $e1 > h1$ ) band ordering. In the limiting cases of small and large fields [corresponding to regions (i) and (iii) in Fig. 1], the system is an insulator (topological and normal, respectively). For intermediate values of  $B$  [region (ii)] there is a partial inversion of the subbands ( $e1 \uparrow > h1 \downarrow > h1 \uparrow > e1 \downarrow$ ). As a result, the electrons move from the  $e1 \uparrow$  subband (filled for  $B = 0$ ) to the  $h1 \uparrow$  subband, which thus becomes the topmost valence subband. And since both heavy-hole subbands are degenerated near  $k = 0$  (see the inset in Fig. 1), the system turns into a semimetallic phase. The gapless phase is therefore the result of both the negligible spin splitting of the heavy-hole states and the large spin splitting of the electron states and can therefore be called a Zeeman semimetal. The quantum phase transitions occur in magnetic fields where the spin-split electron subbands intersect with degenerated hole subbands.

The main factor that drives phase transitions in inverted wells is the large diamagnetic shift of the electron states. Another possibility, presented in Fig. 2(b), is when the well width is smaller than (but close to) the critical value. Then the order of the subbands at  $B = 0$  is normal, but a Zeeman shift under the in-plane field may move the lower of the spin-split electron subbands below the hole subbands. This closes the band gap and converts the system to a semimetallic phase. Only at higher fields is the normal sequence of subbands restored. The semimetallic state is then a purely spin-related phenomenon. When the well width is much smaller than the critical value [Fig. 2(a)], the in-plane field cannot change the order of the subbands and the system remains in the normal insulator state.

As the width of the well increases, the order of the subbands at  $B = 0$  changes, and for  $d > 8.7$  nm, the second holelike subband h2 exceeds the subband e1 and becomes the topmost valence subband as shown in Fig. 3. However, the in-plane field strongly mixes the two subbands, resulting in their anticrossing. Hence, for  $B > 0$  the subband h2 acquires an electronlike character and is holelike only in name. This allows the formation of a gapless semimetallic phase as in narrower wells as shown in Fig. 2(d).

All magnetic-field-driven subband intersections, shown in Fig. 2, are accompanied by a linear dispersion of the intersecting subbands. This is demonstrated in Fig. 4 on the example of a metal-normal insulator transition in a 10-nm well [see also Fig. 2(d)]. The band gap opens here when the light-particle

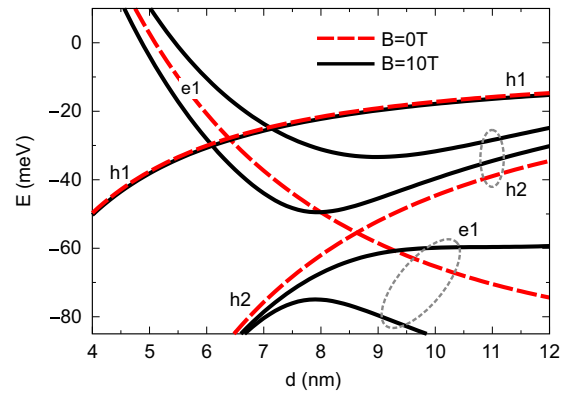


FIG. 3. The  $k = 0$  energies of conduction and valence subbands as functions of the well thickness with and without a magnetic field. The in-plane field does not affect the heavy-hole subband h1, but it strongly mixes the h2 and e1 subbands. As a result, h2 acquires a light-particle character.

subband  $h2 \downarrow$  intersects the heavy-hole subbands h1. More specifically, as shown in Fig. 4(a), the subbands of different spins cross, while those of the same spin anticross. The crossing subbands (i.e.,  $h2 \downarrow$  and  $h1 \uparrow$ ) close to the transition have a Dirac cone spectrum of massless fermions.

Khouri *et al.* [11] studied inverted HgTe quantum wells with a width of 7–11 nm under a strong in-plane magnetic field up to 33 T. In all structures, a negative magnetoresistance was observed at  $B_1 \sim 10$  T, accompanied by the disappearance of nonlocal resistance (in agreement with the results of Gusev *et al.* [8,10]). This effect was explained as a result of the band gap closing by the magnetic field. However, a strong positive magnetoresistance, also detected in all samples at much higher fields ( $B_2 \sim 30$  T), was explained as a classical effect (the high-field property of two-carrier magnetotransport in thin semimetallic crystals [11]). The possibility of reopening the band gap by the strong magnetic field was rejected

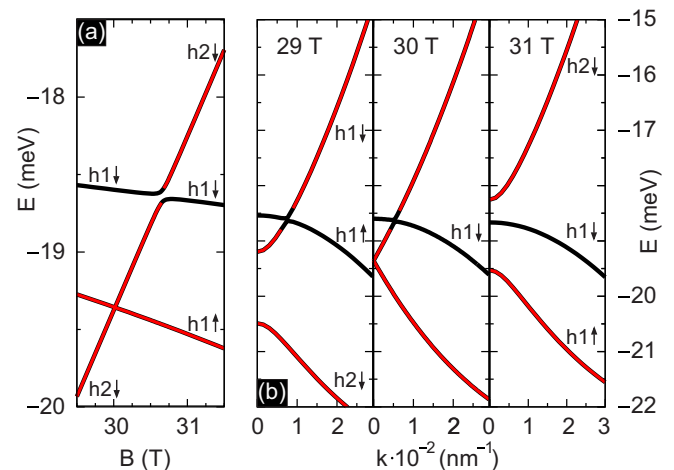


FIG. 4. (a) The enlarged fragment of Fig. 2(d) showing the energies of the subbands in the vicinity of the magnetic-field-induced metal-insulator transition. (b) Subband dispersion at and beyond the phase transition. The intersecting subbands (marked in red) mix and have linear dispersions.

by the authors as inconsistent with the existing theory. Our results allow us to explain the experimental observations in a uniform way: The increasing magnetic field first closes the band gap at  $B = B_1$  and then reopens at  $B = B_2$ , causing two successive phase transitions with an intermediate semimetallic state. For small fields ( $B < B_1$ ) the order of the subbands remains reversed ( $h1 > e1$ ) and the quantum well is in the TI state. On the other hand, strong in-plane fields ( $B > B_2$ ) restore the normal order of the subbands ( $e1 > h1$ ) and drive the system to the NI phase. The band-gap reopening should result in the exponential increase of the resistance, roughly as  $\exp(E_g/k_B T)$ , where the gap  $E_g$  is proportional to the magnetic field. In contrast, the two-carrier model suggested by Khouri *et al.* predicts a power-law increase in resistance. And in one of the studied heterostructures, a linear positive magnetoresistance was indeed observed [11]. But the upturn in resistance observed at  $B = B_2$  in the remaining structures was as steep as its drop at  $B = B_1$ , in line with our theory. Note, however, that Khouri *et al.* observed the reappearance of nonlocal resistance at  $B = B_2$  and attributed this feature to the residual perpendicular component of the magnetic field that acts on the bulk electrons. Our model does not explain this observation.

A quantitative comparison with experiment is difficult because the measured changes in resistance are quite broad (presumably due to the structure inhomogeneity, as discussed in Ref. [10]). Approximately the calculated values of  $B_1$  and  $B_2$  are about 5 T greater than the values measured by Ref. [11]. Thus, our theoretical model describes well the spin splitting of the subbands (which determines the width  $B_2 - B_1$

of the closed-gap region—see Fig. 2), but overestimates the  $B = 0$  band gap in inverted wells. Our calculations also predict that  $B_2$  changes nonmonotonically with increasing well width  $d$ , with a maximum close to  $d \approx 7.5$  nm. A similar trend can be seen in the experimental data (see Fig. 6 in Ref. [11]).

The in-plane magnetic field can be used as a tool for fine tuning the metal-insulator transitions in HgTe quantum wells with  $d \neq d_c$ . In addition, it has an advantage over the previously proposed tools. It was found that the critical thickness  $d_c$  decreases under the influence of the electric field [5] and increases with increasing temperature [7] or hydrostatic pressure [6]. Thus, the electric field can drive the phase transitions only in structures with  $d > d_c$ , while temperature or pressure only in structures with  $d < d_c$ . The in-plane magnetic field works in both cases, provided that the difference  $|d - d_c|$  is small [see Figs. 2(b) and 2(c)].

In conclusion, we have shown that a strong in-plane magnetic field restores the normal band order in the inverted HgTe quantum wells, as the diamagnetic shift of the electron states shifts them above the hole states. This results in two successive phase transitions, first between the topological insulator and the semimetal and then from the semimetal to the normal insulator. The transitions occur when the spin-split electron subbands intersect the magnetic-field-insensitive hole subbands. The intermediate phase between the transitions has semimetallic properties due to the negligible spin splitting of hole states. Both phase transitions have already been observed and the experimental results are in good agreement with our calculations.

- 
- [1] T. Ando, A. B. Fowler, and F. Stern, Electronic properties of two-dimensional systems, *Rev. Mod. Phys.* **54**, 437 (1982).
- [2] B. A. Bernevig, T. L. Hughes, and S.-C. Zhang, Quantum spin Hall effect and topological phase transition in HgTe quantum wells, *Science* **314**, 1757 (2006).
- [3] M. König, S. Wiedmann, C. Brüne, A. Roth, H. Buhmann, L. W. Molenkamp, X.-L. Qi, and S.-C. Zhang, Quantum spin Hall insulator state in HgTe quantum wells, *Science* **318**, 766 (2007).
- [4] B. Büttner, C. X. Liu, G. Tkachov, E. G. Novik, C. Brüne, H. Buhmann, E. M. Hankiewicz, P. Recher, B. Trauzettel, S. C. Zhang, and L. W. Molenkamp, Single valley Dirac fermions in zero-gap HgTe quantum wells, *Nat. Phys.* **7**, 418 (2011).
- [5] W. Yang, K. Chang, and S.-C. Zhang, Intrinsic Spin Hall Effect Induced by Quantum Phase Transition in HgCdTe Quantum Wells, *Phys. Rev. Lett.* **100**, 056602 (2008).
- [6] S. S. Krishtopenko, I. Yahniuk, D. B. But, V. I. Gavrilenko, W. Knap, and F. Teppe, Pressure- and temperature-driven phase transitions in HgTe quantum wells, *Phys. Rev. B* **94**, 245402 (2016).
- [7] A. M. Kadykov, S. S. Krishtopenko, B. Jouault, W. Desrat, W. Knap, S. Ruffenach, C. Consejo, J. Torres, S. V. Morozov, N. N. Mikhailov, S. A. Dvoretzskii, and F. Teppe, Temperature-Induced Topological Phase Transition in HgTe Quantum Wells, *Phys. Rev. Lett.* **120**, 086401 (2018).
- [8] G. M. Gusev, Z. D. Kvon, O. A. Shegai, N. N. Mikhailov, S. A. Dvoretzky, and J. C. Portal, Transport in disordered two-dimensional topological insulators, *Phys. Rev. B* **84**, 121302(R) (2011).
- [9] O. E. Raichev, Effective hamiltonian, energy spectrum, and phase transition induced by in-plane magnetic field in symmetric HgTe quantum wells, *Phys. Rev. B* **85**, 045310 (2012).
- [10] G. M. Gusev, E. B. Olshanetsky, Z. D. Kvon, O. E. Raichev, N. N. Mikhailov, and S. A. Dvoretzky, Transition from insulating to metallic phase induced by in-plane magnetic field in HgTe quantum wells, *Phys. Rev. B* **88**, 195305 (2013).
- [11] T. Khouri, S. Pezzini, M. Bendias, P. Leubner, U. Zeitler, N. E. Hussey, H. Buhmann, L. W. Molenkamp, M. Titov, and S. Wiedmann, Magnetoresistance in the in-plane magnetic field induced semimetallic phase of inverted HgTe quantum wells, *Phys. Rev. B* **99**, 075303 (2019).
- [12] E. O. Kane, Band structure of indium antimonide, *J. Phys. Chem. Solids* **1**, 249 (1957).
- [13] E. G. Novik, A. Pfeuffer-Jeschke, T. Jungwirth, V. Latussek, C. R. Becker, G. Landwehr, H. Buhmann, and L. W. Molenkamp, Band structure of semimagnetic  $\text{Hg}_{1-y}\text{Mn}_y\text{Te}$  quantum wells, *Phys. Rev. B* **72**, 035321 (2005).
- [14] R. Winkler, *Spin-Orbit Coupling Effects in Two-Dimensional Electron and Hole Systems* (Springer, Berlin, 2003).
- [15] T. Skauli and T. Colin, Accurate determination of the lattice constant of molecular beam epitaxial CdHgTe, *J. Cryst. Growth* **222**, 719 (2001).

- [16] J. P. Laurenti, J. Camassel, A. Bouhemadou, B. Toulouse, R. Legros, and A. Lussion, Temperature dependence of the fundamental absorption edge of mercury cadmium telluride, *J. Appl. Phys.* **67**, 6454 (1990).
- [17] A. J. Pfeuffer-Jeschke, Transport experiments in two-dimensional systems with a strong spin-orbit interaction, Ph.D. thesis, Physikalisches Institut, Universität Würzburg, 2000.
- [18] X. C. Zhang, A. Pfeuffer-Jeschke, K. Ortner, V. Hock, H. Buhmann, C. R. Becker, and G. Landwehr, Rashba splitting in *n*-type modulation-doped HgTe quantum wells with an inverted band structure, *Phys. Rev. B* **63**, 245305 (2001).
- [19] W. Kruse, in *Semiconductors and Semimetals*, edited by R. K. Willardson and A. C. Beer (Academic, New York, 1970), Vol. 18, p. 18.
- [20] P. C. Klipstein, Structure of the quantum spin Hall states in HgTe/CdTe and InAs/GaSb/AlSb quantum wells, *Phys. Rev. B* **91**, 035310 (2015).
- [21] K. Takita, K. Onabe, and S. Tanaka, Pressure- and temperature-driven phase transitions in HgTe quantum wells, *Phys. Status Solidi* **92**, 297 (1979).
- [22] See Supplemental Material at <http://link.aps.org/supplemental/10.1103/PhysRevB.104.L161406> for the detailed form of the Kane Hamiltonian and the values of parameters used in the calculations.